Journal of Alloys and Compounds 631 (2015) 298–302

Contents lists available at ScienceDirect

Journal of Alloys and Compounds

journal homepage: www.elsevier.com/locate/jalcom

Visible light photocatalytic synthesis of aniline with an Au/$LaTiO_3$ nanocomposites

I.A. Mkhalid *

Department of Chemistry, Faculty of Science, King Abdulaziz University, PO Box 80203, Jeddah 21589, Saudi Arabia

ARTICLE INFO

Article history:
Received 17 December 2014
Received in revised form 5 January 2015
Accepted 15 January 2015
Available online 23 January 2015

Keywords:
Au
$LaTiO_3$ visible photocatalyst
A reduction of nitrobenzene

ABSTRACT

An ultrasonic method was used to prepare $LaTiO_3$ nanoparticles and a photo-assisted deposition method was used to loading gold into surface of $LaTiO_3$. The samples obtained were characterized using a photo-luminescence emission spectra, X-ray photoelectron spectroscopy, transmission electron microscopy, ultraviolet and visible light spectroscopy, surface area measurements and X-ray diffraction. In addition, photocatalytic activity of $LaTiO_3$ and Au/$LaTiO_3$ samples has been tested under visible light irradiation for reduction of nitrobenzene into aniline. XPS results reveal that gold was present as metallic gold by the presence of two peaks at 87.7 eV and 84.0 eV. The UV–Vis results reveal that loading of Au into $LaTiO_3$ surfaces lead to a red shift. The maximum photocatalytic reduction efficiency (100%) was obtained using 0.3 wt.% Au/$LaTiO_3$ nanocomposites after 90 min a reaction time. The Au/$LaTiO_3$ nanocomposites can be recycled for the first five cycles without loss of photocatalytic activity.

1. Introduction

A process for the catalytic hydrogenation is generally carried out by reduction of nitrobenzene (NB) of aniline in the laboratory and industry, one of the most important and chemical intermediates in the manufacture of pharmaceuticals, dyes, used by, pigments, pesticides, and [1,2]. Transition metals (Cu, Ni) and precious metals (Pt, Pd, Au) are usually prepared as a catalyst [1–3], and the needs of the reaction at a high temperature is used higher than the pressure of H_2, and a length greater met, a aniline achieve selectivity [3,4]. Induced photochemical reduction of nitrobenzene, aniline, which can be produced at room temperature using a photocatalyst is of great scientific value and raises many attentions to continue [5–7], the synthesis of environmentally friendly or green. Although the reduction of nitrobenzene (NB) and the aniline derivative of the photocatalytic technology in Refs. [5,8–10], the conversion and the selectivity are low, and [8,11–14]. TiO_2 can be activated by UV light. This means that only about 3–5% of the light of the solar spectrum may be used by TiO_2. Are developed from the standpoint encouraged the use of solar energy into visible light has photo. A semiconductor photocatalyst, the negative value of the conduction band, the largest reduction in the activity must be provided. In theory, when the potential of the conduction band of a photocatalyst is lower than −0.486 V can nitrobenzene to aniline image (E ($C_6H_5NO_2/C_6H_5NH_2$) = −0.486 V [15] can be reduced, compared to NHE). Therefore, the construction of new semiconductor image narrow band gap, high negative values of the conduction band is to be an effective method for reducing NB. TiO_2 is the most popular material for this method due to the higher photocatalytic activity, good photostability, non-toxicity and low cost. However, the large band gap of TiO_2, which is 3.2 eV, has proven to be a significant disadvantage; the wavelengths below 400 nm are required for excitation, which limits the efficiency of the solar light source. Therefore, the change of the band gap of TiO_2 is useful for improving the optical properties of this material. In recent decades, doping has been successfully used by metals and non-metals to move the optical response of the catalytic activity of TiO_2 from UV to visible light [16,17].

Remarkable progress in the development of photocatalysts, as $NaTaO_3$ [17–21] $K_2La_2Ti_3O_{10}$ [22] and $SrTiO_3$ [23] produced. Of these photocatalysts $LaTiO_3$ is extensively due to their high photocatalytic activity in water splitting stoichiometric H_2 and O_2 under investigation [17]. However, these photocatalysts work only under ultraviolet light, which accounts for only 4% of the solar energy. On the other hand, more than 40% of solar energy visible light. As a result, the visible light photocatalysts pulled Leads more attention in recent years [24–27]. Doping has been shown previously that one method for the production of visible light photo driven. In general, the band structure of doping semiconductors [24,25,28] and influences the structure of the grain size and the surface of materials, which are generally a better photocatalytic activity [17]. In this study, we illustrate the synthesis of Au/$LaTiO_3$ Au/$LaTiO_3$ nanocomposites. The photocatalytic performance of Au/$LaTiO_3$

* Tel.: +966 2 640000; fax: +966 2 6952292.
E-mail address: imkhalid2@gmail.com

http://dx.doi.org/10.1016/j.jallcom.2015.01.101
0925-8388/

$Au/LaTiO_3$ nanocomposites was studied for synthesis of aniline from photocatalytic reduction of nitrobenzene.

2. Experimental

2.1. Preparation of photocatalyst

$LaTiO_3$ nanoparticles are prepared by an ultrasonic method. All of the chemicals were used without further purification. In a typical preparation, 0.3 mol of lanthanum acetate was added under a nitrogen atmosphere to 16 mol of glacial acetic acid and stirred for 2 h at room temperature. Then, 5 mol of titanium isoperoxide, was added to above solution and the resulting mixture was stirred at room temperature for 6 h. Then, 20 ml of acetone was added to them and the resulting mixture was put in an apparatus for low frequency ultrasound (Bransonic 42 kHz) for 1 h. The resulting materials were dried for 24 h at 100 °C, and then the materials were calcined at 550 °C for 5 h in air. A photo-assisted deposition (PAD) route was used to prepare $Au/LaTiO_3$ samples which contain different wt.% from Au metal (0.1, 0.2, 0.3, and 0.4 wt.%). In this route, Au metal was deposited on $LaTiO_3$ under UV-light irradiation by using an aqueous solution of $HAuCl_4$. The obtained samples dried for 24 h at 60 °C.

2.2. Characterization of photocatalysts

Bruker axis D8 with Cu Kα radiation (λ = 1.540 Å) is used for X-ray diffraction (XRD) analysis that was done at room temperature. N_2-adsorption measurements were used for calculating the surface area and for that purpose a Nova 2000 series Chromatech apparatus at 77 K was used. The samples were treated for 2 h under vacuum at 100 °C before taking the measurements. A UV–visible diffuse reflectance spectroscopy (UV–Vis-DRS) is used for displaying the performance of the band-gap of samples. The spectroscopy is done in air at room temperature using a UV/Vis/NIR spectrophotometer (V-570, JASCO, Japan) and in the wavelength range of 200–800 nm. A JEOL-JEM-1230 microscope is used for conducting the transmission electron microscopy (TEM). The entire samples were set up in a suspension of ethanol and then for half an hour of ultrasonication are done over the samples. A low amount of solution is placed on a copper grid coated by carbon and left to dry. Once the solution is dry, the sample is loaded into the TEM. A Thermo Scientific K-ALPHA, XPS is used for performing the X-ray photoelectron spectroscopy (XPS). Photoluminescence (Pl) emission spectra was measured by Shimadzu RF-5301 fluorescence spectrophotometer.

2.3. Photocatalytic performance

The photocatalytic apparatus consists of two parts: a sealed quartz reactor and an annular quartz tube. A visible light source is obtained by a 500-W Xenon lamp (Institute of Electric Light Source, Beijing) with a maximum emission of about 470 nm and cutoff filter to control wavelength of light. The lamp was in an empty chamber of the annular tube, and running water passed through the tub and continuous cooling kept the temperature of reaction solution at approximately 30 °C. The sealed quartz reactor has a diameter of 8.3 cm and is put below the lamp. 50 mg of photocatalyst was dispersed in 10 ml of nitrobenzene-CH_3OH mixture (1/99, v/v), where 8.13×10^{-4} mol/L is initial concentration of nitrobenzene. 11 cm is the distance between the surface of reaction solution and light source. Before illumination, dissolved oxygen in reaction mixture was removed by passing nitrogen gas through the reaction mixture for 30 min. At interval times, samples which were taken from reaction mixture were filtrated to remove any residual particles and the filtrates were analyzed using a gas chromatography Agilent GC 7890A model: G3440A Gas Chromatography using 19091J-413 capillary column (30 m × 0.32 μm × 0.25 μm).

2.4. Structural characterization, morphology and composition

The X-ray diffraction patterns of $LaTiO_3$ and $Au/LaTiO_3$ $Au/LaTiO_3$ nanocomposites are compared in Fig. 1. The structural feature of $LaTiO_3$ and $Au/LaTiO_3$ $Au/LaTiO_3$ nanocomposites are mainly composed of $LaTiO_3$ (JCPDS card: 75-0267), indicating that the $LaTiO_3$ structure remained after doping of Au into surface of $LaTiO_3$ by PAD method. However, no diffraction peaks for Au or Au_2O was appeared, due to low weight percent of gold or may be Au is well dispersed into surface of $LaTiO_3$. Also, we noticed that dispersion of Au into surface of $LaTiO_3$ leads to decrease peak intensity of XRD. The average crystallite size of $LaTiO_3$ was calculated by Scherer equation using the half-width of the peak in the X-ray diffraction pattern at $2\theta = 32.07°$, which corresponds to the most intense peak. The crystallite size of $LaTiO_3$, 0.1 wt.% $Au/LaTiO_3$, 0.2 wt.% $Au/LaTiO_3$, 0.3 wt.% $Au/LaTiO_3$, and 0.4 wt.% $Au/LaTiO_3$ $Au/LaTiO_3$ nanocomposites were 35, 30, 23, 18 and 14 nm, respectively. Thus, the crystallite size of $LaTiO_3$ was decreased by increase weight percent of doped gold.

XPS spectra of 0.3 wt.% $Au/LaTiO_3$ nanocomposite is shown in Fig. 2. XPS spectra showed that the peak at 87.7 eV and 84.0 eV attributed to metallic gold, which confirm that gold is dispersed above $LaTiO_3$ surface as gold metal.

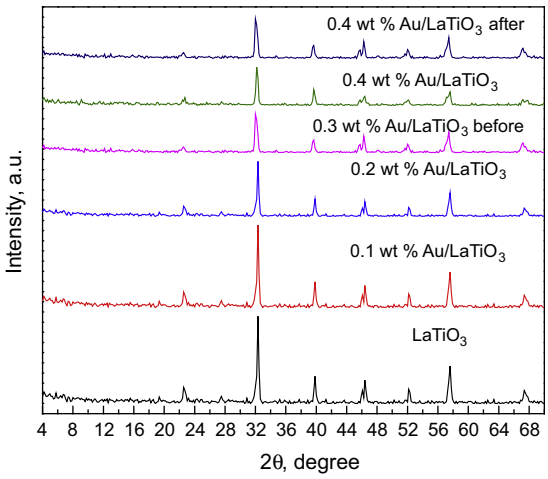

Fig. 1. XRD pattern of $LaTiO_3$ and $Au/LaTiO_3$ nanocomposites.

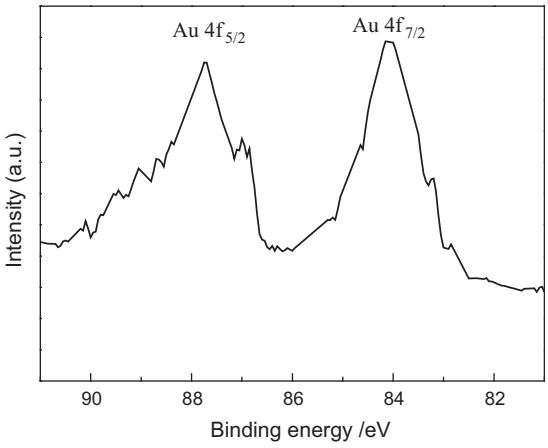

Fig. 2. XPS spectra of Au 4f for 0.3 wt.% $Au/LaTiO_3$ nanocomposites.

TEM images of $LaTiO_3$ and $Au/LaTiO_3$ nanocomposites are shown in Fig. 3. The results reveal that the gold is well dispersed into $LaTiO_3$ surface, and the diameter of the gold depend on weight percent of gold. It is clear that the homogeneity of gold was increased by increase weight percent of gold up to 0.3 wt.%. In addition, higher weight percent of gold (i.e. 0.4) decreases the homogeneity. This observation indicated that there is an optimum value for the deposition of gold metal.

2.5. Texture structure

The texture parameters of $LaTiO_3$ and $Au/LaTiO_3$ nanocomposites are demonstrated in Table 1. The S_{BET} values for $LaTiO_3$, 0.1 wt.% $Au/LaTiO_3$, 0.2 wt.% $Au/LaTiO_3$, 0.3% $Au/LaTiO_3$ and 0.4% $Au/LaTiO_3$ nanocomposites were 19, 18, 15, 13 and 11 m^2/g, respectively. The total pore volume of $Au/LaTiO_3$ is smaller than that of $LaTiO_3$ sample due to the blocking of some pore of $Au/LaTiO_3$ by Au metal deposition. Presence of mesopores in all samples was confirmed by close values of S_{BET} and S_t in most samples as shown in Table 1.

2.6. Optical characterization

UV–Vis diffuse reflectance spectra of $LaTiO_3$ and $Au/LaTiO_3$ nanocomposites is shown in Fig. 4. The results reveal that the absorption edge of $LaTiO_3$ was shifted from 427.6 to 539.1 nm by deposition of Au metal into $LaTiO_3$ surface. The results of UV–Vis spectra's were used to calculate direct band gap of $LaTiO_3$ and $Au/LaTiO_3$ nanocomposites based on the method which used by Kumar et al. [29]. The band gap energies were calculated employing the following equation:

$$E_g = 1239.8/\lambda$$

where λ is wavelength of the absorption edges in the spectrum (nm), and E_g is band gap (eV). The results are tabulated in Table 2. The results reveal that the band gap was decreased from 3.4 to 2.4 eV by increase wt.% of Au from 0.1 to 0.3 wt.%, respectively. However, no significant change in the band gap is found by high wt.% of Au above 0.30. Therefore, band gap was controlled by control wt.% of Au deposited.

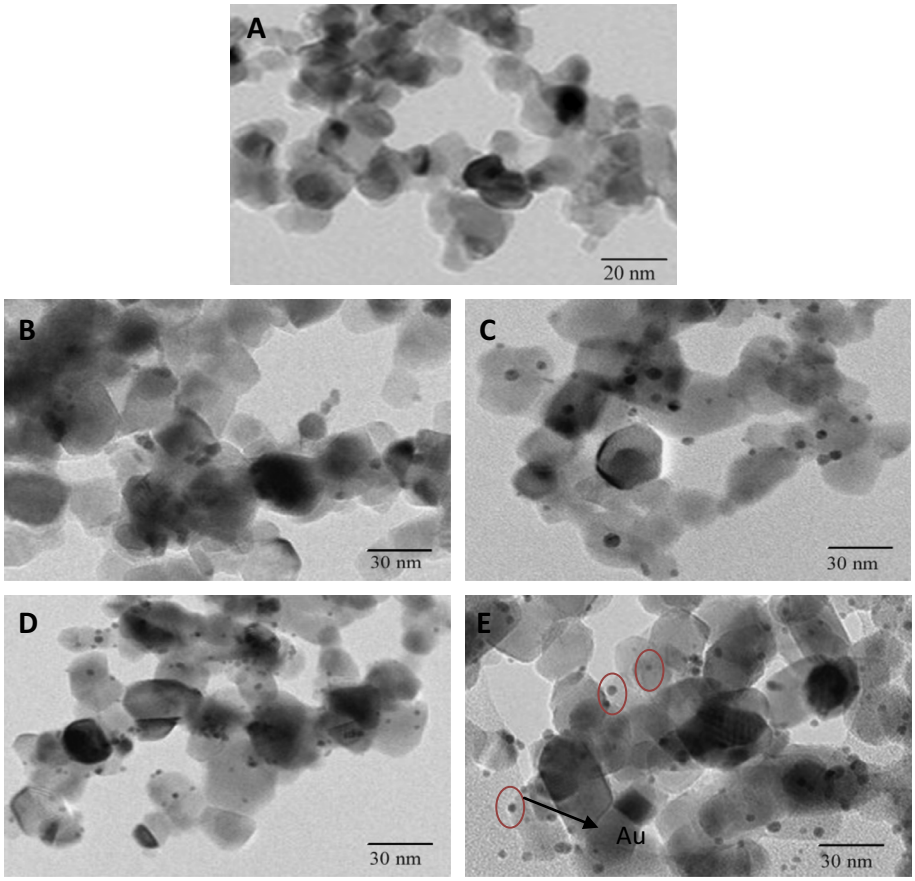

Fig. 3. TEM images of $LaTiO_3$ and $Au/LaTiO_3$ nanocomposites, where wt.% of Au is 0.0 (A), 01 (B), 0.2 (C), 0.3 (D) and 0.4 (E).

Table 1
Texture parameters of $LaTiO_3$ and $Au/LaTiO_3$ nanocomposites.

Sample	S_{BET} (m^2/g)	S_t (m^2/g)	S_{micro} (cm^2/g)	S_{ext} (cm^2/g)	V_p (cm^3/g)	V_{micro} (cm^3/g)	V_{meso} (cm^3/g)	r (Å)
$LaTiO_3$	19	20	13	6	0.160	0.125	0.035	45.00
0.1 wt.% $Au/LaTiO_3$	18	19	12	5	0.105	0.087	0.018	48.00
0.2 wt.% $Au/LaTiO_3$	15	16	11	4	0.077	0.067	0.015	52.00
0.3 wt.% $Au/LaTiO_3$	13	14	10	3	0.070	0.62	0.013	55.00
0.4 wt.% $Au/LaTiO_3$	11	12	9	2	0.048	0.042	0.011	58.00

Note:
(S_{BET}) – BET surface area, (S_t) – surface area derived from V_{l-t} plots.
(S_{micro}) – surface area of micropores, (S_{ext}) – external surface area.
(V_p) – total pore volume, (V_{micro}) – pore volume of micropores.
(V_{meso}) – pore volume of mesopores, (r^-) – mean pore radius.

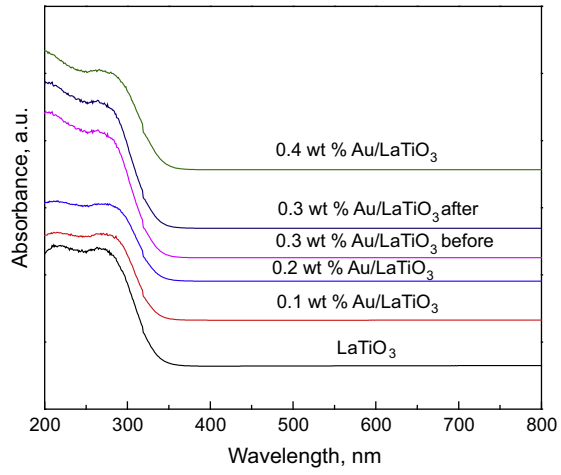

Fig. 4. UV–Vis absorption spectra of $LaTiO_3$ and $Au/LaTiO_3$ nanocomposites.

Photoluminescence (Pl) emission spectra were used to study and understand the separation and recombination of electron and holes. The Pl spectra of the various samples which excited at 265 nm at room temperature are shown in Fig. 5. The intensity of the Pl is greatly reduced with increase weight% of Au.

2.7. Photocatalytic measurements

Photocatalytic performance of $LaTiO_3$ and $Au/LaTiO_3$ nanocomposites were tested by examining the photocatalytic reduction of nitrobenzene (NB) to aniline (AN) using visible light irradiation. Nitrosobenzene and aniline are the main components, which are detected by gas chromatography (GC). There is no evidence of aniline or nitrosobenzene in the absence of light or a catalyst. Fig. 6 shows a photocatalytic reduction of nitrobenzene by TiO_2 Degussa, $LaTiO_3$ and $Au/LaTiO_3$ nanocomposites. The results show that the TiO_2 Degussa has a very low photocatalytic activity, because TiO_2 Degussa absorb in the UV region, and the photocatalytic reaction was carried out under visible light. In addition, the following sequence of photocatalytic activity: $LaTiO_3$ < 0.1% $Au/LaTiO_3$ < 0.2% $Au/LaTiO_3$ < 0.4% $Au/LaTiO_3$ < 0.3% $Au/LaTiO_3$. Therefore, weight percent of gold was controlled photocatalytic activity of $LaTiO_3$. Furthermore, the photocatalytic activity of 0.4% $Au/LaTiO_3$ is less than that 0.3% $Au/LaTiO_3$. Because high weight percent of gold can act as the center of recombination for electron and hole pair, and thus reduce the photocatalytic activity.

Table 2
Band gap energy of $LaTiO_3$ and $Au/LaTiO_3$ nanocomposites.

Sample	Band gap energy, eV
$LaTiO_3$	3.6
0.1 wt.% $Au/LaTiO_3$	3.1
0.2 wt.% $Au/LaTiO_3$	2.8
0.3 wt.% $Au/LaTiO_3$	2.6
0.4 wt.% $Au/LaTiO_3$	2.4

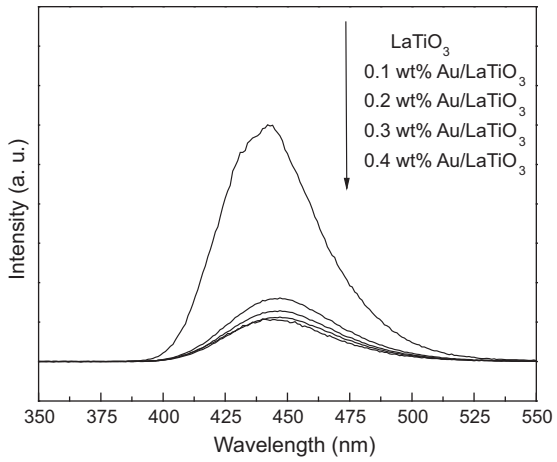

Fig. 5. Pl spectra of $LaTiO_3$ and $Au/LaTiO_3$ nanocomposites.

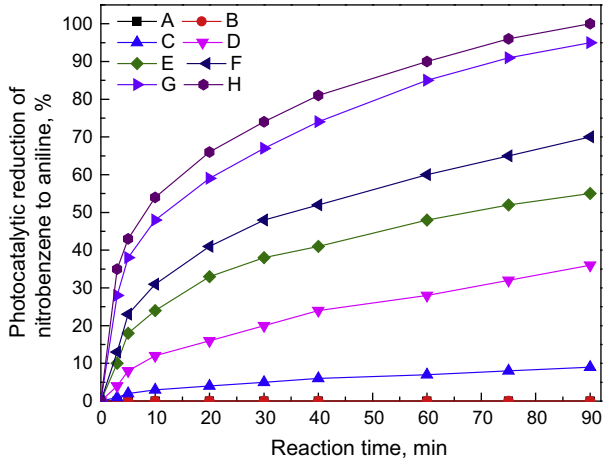

Fig. 6. Photocatalytic reduction of nitrobenzene to aniline, % by no catalyst (A), no light (B), TiO_2 Degussa (C), $LaTiO_3$ (D), 0.1 wt.% $Au/LaTiO_3$ (E), 0.2 wt.% $Au/LaTiO_3$ (F), 0.3 wt.% $Au/LaTiO_3$ (G) and 0.4 wt.% $Au/LaTiO_3$ (H).

2.8. Photochemical stability

Fig. 7 shows the results obtained regarding the recycling and reuse of photocatalysts for the photocatalytic reduction of nitrobenzene solution. The experiment was carried out under the following conditions: a reaction time of 90 min, a nitrobenzene solution concentration of 8.13×10^{-4} mol/L and 50 mg of 0.3% wt.% $Au/LaTiO_3$ nanocomposites. Fig. 7 shows photocatalytic reduction of nitrobenzene to aniline by 0.3 wt.% $Au/LaTiO_3$ after reuse five times. The results reveal that photocatalytic reduction of nitrobenzene after being reused five times almost remains unchanged. The XRD patterns of the 0.3% wt.% $Au/LaTiO_3$ nanocomposite obtained before and after being reused five times are shown in Fig. 1. It was also observed that the shape of the composite XRD patterns after the first five cycles was similar to the shape observed before the reaction. This finding indicates that the structure of the 00.3% wt.% $Au/LaTiO_3$ does not change during the photocatalytic process. In addition, the UV–Vis spectra of the 0.3% wt.% $Au/LaTiO_3$ sample before and after being reused five times are shown in Fig. 4. It was also observed that the absorption spectrum of the 0.3% wt.% $Au/LaTiO_3$ sample after the first five cycles was similar to that observed before the reaction. This result indicates that the structure of 0.3% wt.% $Au/LaTiO_3$ does not change during the photocatalytic process. Therefore, this photocatalyst can be separated and recycled while maintaining its stability, making it a promising material for environmental remediation.

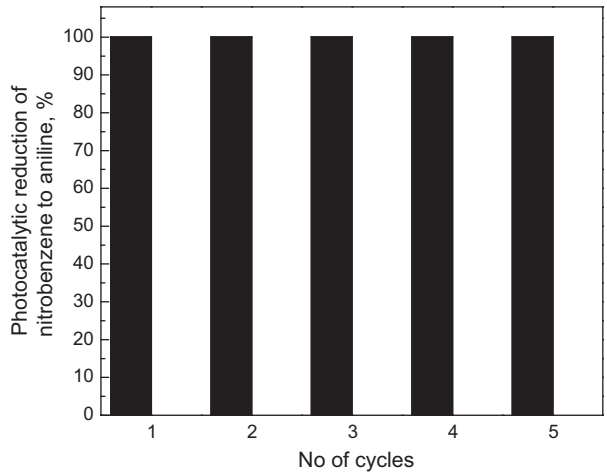

Fig. 7. Recycle and reuse of 0.3 wt.% $Au/LaTiO_3$ photocatalysts for nitrobenzene photocatalytic reduction.

2.9. Mechanisms

Nitrosobenzene and aniline are the main compounds, which are detected by gas chromatography (GC). Photocatalytic reduction of nitrobenzene over 0.3 wt.% $Au/LaTiO_3$ nanocomposites can be discussed as the following: (1) Irradiation of 0.3 wt.% $Au/LaTiO_3$ nanocomposites by visible light cause generation of e–h pairs, as shown in Eq. (1); (2) moving of generated electron and holes to surface of photocatalyst; (3) production of reductive H as shown in Eqs. (2) and (3); and (4) producing of aniline as the final product and nitrosobenzene as the intermediate, as shown in Eq. (4).

$$Au/LaTiO_3 \xrightarrow{\text{Visible light}} Au/LaTiO_3\ (e^- + h^+) \quad (1)$$

$$CH_3OH + h^+ \longrightarrow CH_3O^{\cdot} + {}^{\cdot}CH_2OH \quad (2)$$

$$CH_3O^{\cdot} + {}^{\cdot}CH_2OH \rightarrow 2H^{\cdot} + 2HCHO \quad (3)$$

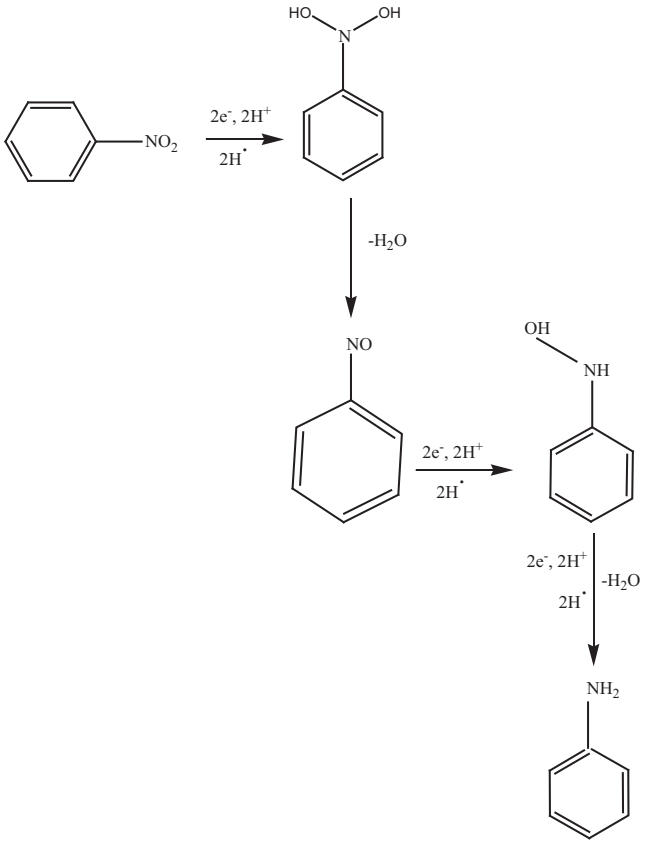

(4)

3. Conclusions

Au/$LaTiO_3$ nanocomposites, which were prepared by an ultrasonic method, are promising photocatalysts under visible light and have a high performance for the removal of pollutants and organic synthesis. The doping of gold lead to shift absorption edge to longer wavelengths and the shift of absorption edge to longer wavelength was increases directly with wt.% of doped gold. Results of photocatalytic activity reveal that 0.3 wt.% Au/$LaTiO_3$ nanocomposites is the most active photocatalyst for the reduction of nitrobenzene under visible light. The 100% yield of photocatalytic reduction of nitrobenzene was obtained under the following conditions: 50 mg weight of 0.3 wt.% Au/$LaTiO_3$; 90 min irradiation time; Xenon lamp irradiation source; and 8.13×10^{-4} mol/l concentration of nitrobenzene. Also, 0.3 wt.% Au/$LaTiO_3$ nanoparticle has high photocatalytic stability after reused five times.

Acknowledgements

This work was funded by the Deanship of Scientific Research (DSR), King Abdulaziz University, Jeddah, under grant number (130-67-D1435). The authors, therefore, acknowledge with thanks DSR technical and financial support.

References

[1] A. Corma, P. Concepcion, P. Serna, Angew. Chem. Int. Ed. 46 (2007) 7266–7269.
[2] J. Wang, Z. Yuan, R. Nie, Z. Hou, X. Zheng, Ind. Eng. Chem. Res. 49 (2010) 4664–4669.
[3] S.-P. Lee, Y.-W. Chen, J. Mol. Catal. A: Chem. 152 (2000) 213–223.
[4] H. Li, Q. Zhao, Y. Wan, W. Dai, M. Qiao, J. Catal. 244 (2006) 251–254.
[5] S.O. Flores, O. Rios-Bernij, M.A. Valenzuela, I. Córdova, R. Gómez, R. Gutiérrez, Top. Catal. 44 (2007) 507–511.
[6] S. Fuldner, P. Pohla, H. Bartling, S. Dankesreiter, R. Stadler, M. Gruber, A. Pfitzner, B. Konig, Green Chem. 13 (2011) 640–643.
[7] J.L. Ferry, W.H. Glaze, Langmuir 14 (1998) 3551–3555.
[8] S. Chen, H. Zhang, X. Yu, W. Liu, Chin. J. Chem. 28 (2010) 21–26.
[9] F. Mahdavi, T.C. Bruton, Y. Li, J. Org. Chem. 58 (1993) 744–746.
[10] J.L. Ferry, W.H. Glaze, J. Phys. Chem. B 102 (1998) 2239–2244.
[11] G. Liu, X. Li, J. Zhao, S. Horikoshi, H. Hidaka, J. Mol. Catal. A: Chem. 153 (2000) 221–229.
[12] H.-P. Dai, K.-K. Shiu, Electrochim. Acta 43 (1998) 2709–2715.
[13] S.D. Rychnovsky, R. Vaidyanathan, T. Beauchamp, R. Lin, P.J. Farmer, J. Org. Chem. 64 (1999) 6745–6749.
[14] M. Zhang, C. Chen, W. Ma, J. Zhao, Angew. Chem. Int. Ed. 120 (2008) 9876–9879.
[15] S. Balasubramanian, J. Lumin. 106 (2004) 69–76.
[16] R.M. Mohamed, A.A. Ismail, I. Othman, I.A. Ibrahim, J. Mol. Catal. A: Chem. 238 (2005) 151–161.
[17] H. Kato, K. Asakura, A. Kudo, J. Am. Chem. Soc. 125 (2003) 3082–3089.
[18] D.G. Porob, P.A. Maggard, J. Solid State Chem. 179 (2006) 1727–1732.
[19] A. Iwase, H. Kato, A. Kudo, Chem. Sus. Chem. 2 (2009) 873–877.
[20] M. Maruyama, A. Iwase, H. Kato, A. Kudo, H. Onishi, J. Phys. Chem. C 113 (2009) 13918–13923.
[21] T. Takata, K. Shinohara, A. Tanaka, M. Hara, J.N. Kondo, K. Domen, J. Photochem. Photobiol. A 106 (1997) 45–49.
[22] K. Domen, A. Kudo, T. Onishi, J. Phys. Chem. 90 (1986) 292–295.
[23] R. Asahi, T. Morikawa, T. Ohwaki, K. Aoki, Y. Taga, Science 293 (2001) 269–271.
[24] Z.G. Zou, J.H. Ye, K. Sayama, H. Arakawa, Nature 414 (2001) 625–627.
[25] K. Maeda, K. Teramura, D.L. Lu, T. Takata, N. Saito, Y. Inoue, K. Domen, Nature 440 (2006). 295–295.
[26] Z.G. Yi, J.H. Ye, Appl. Phys. Lett. 91 (2007) 254108–254110.
[27] X.C. Wang, K. Maeda, A. Thomas, K. Takanabe, G. Xin, J.M. Carlsson, K. Domen, M. Antonietti, Nat. Mater. 8 (2009) 76–80.
[28] D.W. Hwang, H.G. Kim, J.S. Lee, J. Kim, W. Li, S.H. Oh, J. Phys. Chem. B 109 (2005) 2093–2102.
[29] V. Kumar, S.K. Sharma, T.P. Sharma, V. Singh, Opt. Mater. 12 (1999) 115–119.